DOI: 10.1002/ejic.201100627

Mono- and Dinuclear Co/Ni Complexes Bearing Redox-Active Tetrathiafulvaleneacetylacetonate Ligands – Syntheses, Crystal Structures, and Properties

Jing Xiong,[a] Gao-Nan Li,[a] Lei Sun,[a] Yi-Zhi Li,[a] Jing-Lin Zuo,*[a] and Xiao-Zeng You[a]

Keywords: Cobalt / Nickel / Ligand design / Charge transfer / Polynuclear complexes / Density functional calculations

A series of tetrathiafulvalene-substituted acetylacetonate ligands (**L_1**–**L_4**) has been synthesized and characterized. Reaction of the ligands with (Tp^{Ph_2})Co(OAc)(Hpz^{Ph_2}) and (Tp^{Ph_2})-Ni(OAc) [Tp^{Ph_2} = hydrotris(3,5-diphenylpyrazol-1-yl)borate; Hpz^{Ph_2} = 3,5-diphenylpyrazole] afforded eight new mono- or dinuclear complexes **1**–**8**: $Tp^{Ph_2}M\mathbf{L_1}$ or $(Tp^{Ph_2}M)_2\mathbf{L}$ (M = Co, Ni; **L** = **L_2**, **L_3** and **L_4**). The crystal structures of **L_4** and **1**–**3**, **5**, and **6** were determined by X-ray crystallography. The absorption spectra and redox behavior of these compounds have been studied. The optimized geometry and electron absorption spectrum of **2** were analyzed by DFT and time-dependent (TD)-DFT.

Introduction

Over the last decade, much attention has been focused on searching for new multifunctional molecular materials.[1] In particular, molecular magnetic semiconductors or conductors that possess synergy or interplay between electrical conductivity and magnetism have attracted increasing interest.[1–2] A strategy for these materials is to establish coupling between conduction electrons (π electrons) from organic donors and localized electrons (d electrons) from paramagnetic centers, and these materials are called "π–d systems". As an organic donor, tetrathiafulvalene (TTF) and its derivatives have long been known as essential building blocks for the preparation of organic conductors and superconductors.[3] To achieve materials with intriguing structures and interesting properties, a variety of mono- and polydentate coordinating functional groups, such as dithiolate,[4–7] pyridine,[8–9] N-heterocycle,[10–11] phosphane,[12] carboxylate,[13] acetylacetonate,[14] and Schiff base,[15] have been reported as covalent linkages between redox active TTF units and transition metal ions. The appropriate ligands are important and they can act as effective bridges to link the paramagnetic centers and conducting electrons. It is expected that such direct connection will provide possible communication between the inorganic and organic substructures in order to modify or enhance their properties such as conductivity, magnetic, photophysical, and photochemical properties.

Tris(pyrazolyl)borate (Tp) anions are popular ligands used in coordination chemistry[16] because of their easy preparation and unique steric and electronic properties. With the discovery of second generation scorpionates by Trofimenko, Tp^{tBu}, Tp^{Ph}, and Tp^{iPr} half-sandwich complexes [Tp^RCoX] (X = halide or pseudohalide) have become available.[17] Recently, complexes with Tp have been developed as polymerization catalysts, spectroscopic probes, and molecular magnets.[18]

In previous studies, the acetylacetonate group has been successfully connected to the TTF skeleton[14] and some TTF-based mono- and bis(acetylacetonate) ligands (**L_1** and *trans*-$acac_2$ in Scheme 1) have also been reported.[14d] In this paper, new ligands with two acetylacetonate groups linked to the same side of the TTF moiety (**L_2**–**L_4**, Scheme 1) are reported. Reaction of **L_1**–**L_4** with (Tp^{Ph_2})Co(OAc)(Hpz^{Ph_2}) and (Tp^{Ph_2})Ni(OAc) afford complexes **1**–**8**, respectively (Scheme 2). The spectroscopic and electrochemical properties of these new compounds have been studied, and the structures of some typical complexes are described.

Results and Discussion

Synthesis and Characterization

As shown in Scheme 2, the reaction of tetrathiafulvalene-substituted thiapropanenitrile precursors with 3-chloro-2,4-pentanedione afforded tetrathiafulvalenyl-acetylacetonate ligands **L_2**–**L_4**, which are soluble in most organic solvents and are air-stable in both solution and the solid state. In

[a] State Key Laboratory of Coordination Chemistry, School of Chemistry and Chemical Engineering, Nanjing National Laboratory of Microstructures, Nanjing University, Nanjing 210093, P. R. China
Fax: +86-25-83314502
E-mail: zuojl@nju.edu.cn

Supporting information for this article is available on the WWW under http://dx.doi.org/10.1002/ejic.201100627.

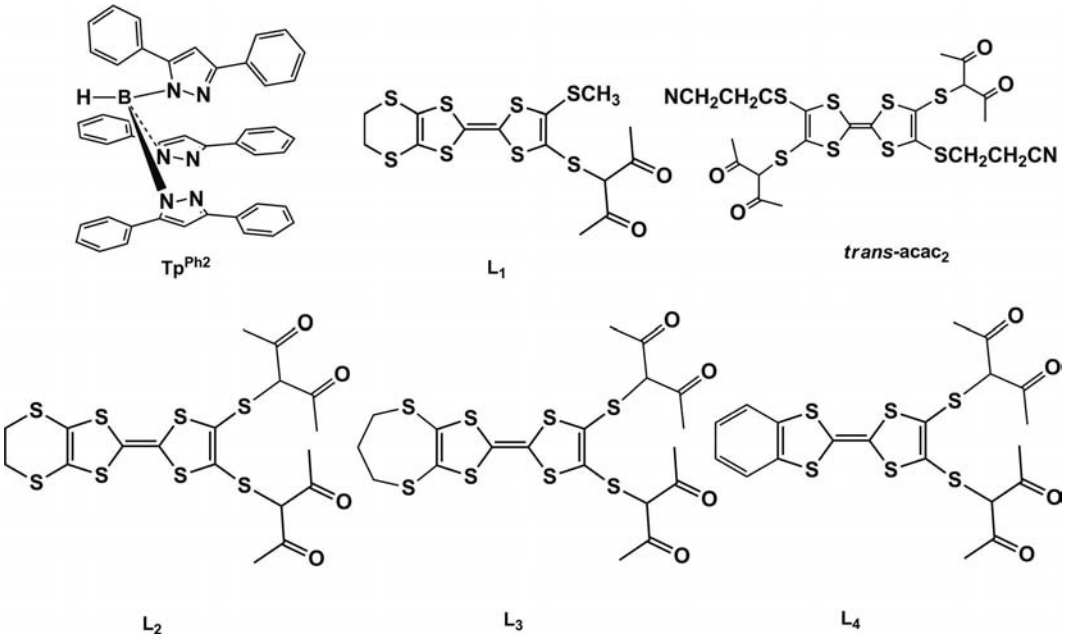

Scheme 1. Structures of Tp^{Ph_2}, *trans*-$acac_2$, and $\mathbf{L_1}$–$\mathbf{L_4}$.

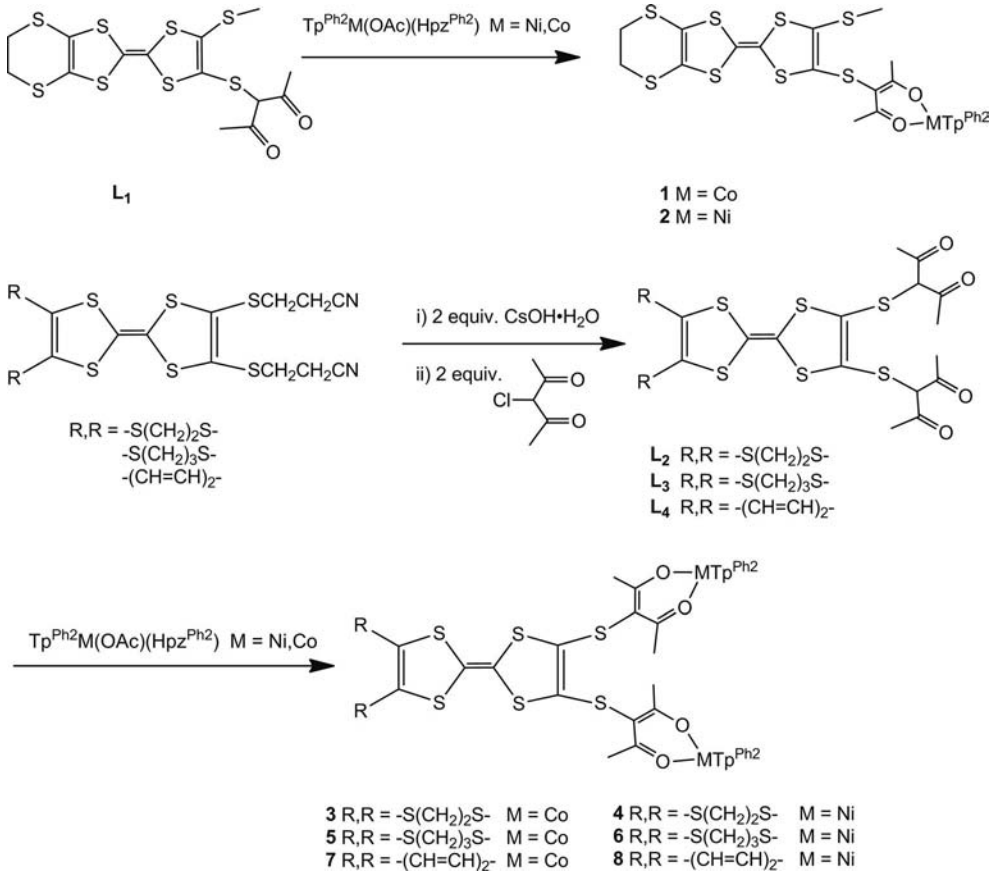

Scheme 2. Synthetic routes to **1**–**8**.

the ^{1}H NMR spectra of $\mathbf{L_1}$–$\mathbf{L_4}$, the presence of a singlet peak (ca. 17.25 ppm) arising from acetylacetonate indicates the keto–enol tautomerism of the ligands. Complexes **1**–**8** show sharp absorption bands at around 1567 and 1477 cm^{-1} in their IR spectra, which are indicative of β-diketonate moieties chelating to the metal ions.[14a,14b,19] Thermogravimetric analysis (TGA) of **1** showed the first weight loss at 139 °C, which corresponds approximately to

the loss of solvent molecules. Complete decomposition occurs at around 265 °C. Among the Co^{II} complexes, **5** is the most stable and decomposed at 304 °C (Figure 1).

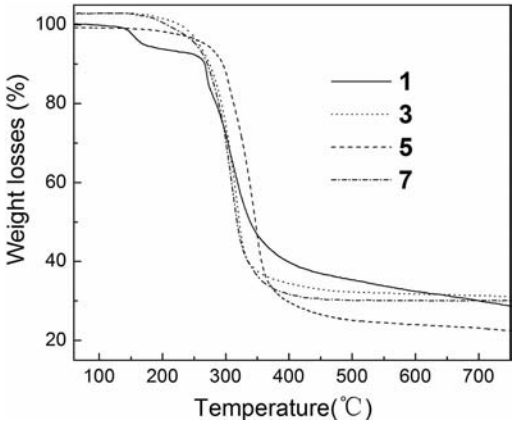

Figure 1. TGA curves for **1**, **3**, **5**, and **7**.

Crystal Structures

The solid-state structures of $\mathbf{L_4}$, **1**–**3**, **5**, and **6** were determined by single-crystal X-ray diffraction. The crystallographic and data collection parameters are given in Table 1; selected bond lengths and angles are listed in Tables 2, 3, 4, and S1–S3.

Figure 2 gives the ORTEP view of $\mathbf{L_4}$. The TTF core and the phenyl ring are nearly planar and almost perpendicular to the plane formed by the acetylacetonate group with a dihedral angle of 85.5°. The bond lengths within the two acetylacetone groups are quite different: 1.273(5) and 1.330(5) Å for C2–O1 and C4–O2, and 1.421(6) and 1.354(6) Å for C2–C3 and C3–C4, respectively. These data

Table 2. Selected bond lengths [Å] and angles [°] for $\mathbf{L_4}$.

Bond			
C(1)–C(2)	1.479(6)	C(4)–C(5)	1.488(6)
C(2)–O(1)	1.273(5)	C(4)–O(2)	1.330(5)
C(3)–S(1)	1.760(4)	C(11)–S(1)	1.786(4)
C(11)–C(12)	1.320(5)	C(15)–C(20)	1.3900
C(16)–C(17)	1.3900	C(13)–C(14)	1.347(5)
O(1)–C(2)–C(3)	118.9(4)	O(2)–C(4)–C(3)	119.0(4)
C(3)–S(1)–C(11)	101.79(18)	C(12)–C(11)–S(1)	121.0(3)

Table 3. Selected bond lengths [Å] and angles [°] for **2**.

Bond			
B(1)–N(2)	1.566(4)	B(1)–N(4)	1.541(4)
B(1)–N(6)	1.521(4)	N(1)–Ni(1)	2.053(3)
N(3)–Ni(1)	2.010(3)	N(5)–Ni(1)	2.054(2)
Ni(1)–O(1)	1.951(2)	Ni(1)–O(2)	1.958(2)
C(53)–C(54)	1.328(6)	C(48)–S(7)	1.759(3)
O(1)–Ni(1)–O(2)	89.13(9)	O(1)–Ni(1)–N(3)	98.89(10)
N(1)–Ni(1)–N(5)	87.18(10)	N(3)–Ni(1)–N(5)	91.73(9)

Table 4. Selected bond lengths [Å] and angles [°] for **6**.

Bond			
B(1)–N(2)	1.540(4)	B(1)–N(6)	1.549(4)
B(1)–N(4)	1.550(4)	Ni(1)–N(1)	2.024(3)
Ni(1)–N(5)	2.054(3)	Ni(1)–N(3)	2.069(2)
Ni(1)–O(1)	1.963(2)	Ni(1)–O(2)	1.981(2)
O(1)–Ni(1)–O(2)	86.78(9)	O(1)–Ni(1)–N(1)	103.04(9)
N(1)–Ni(1)–N(5)	88.37(10)		

Table 1. Crystallographic data for $\mathbf{L_4}$ and **1**–**3**, **5**, and **6**.

	$\mathbf{L_4}$	**1**	**2**	**3**	**5**	**6**
Empirical formula	$C_{20}H_{18}O_4S_6$	$C_{236}H_{188}B_4Co_4N_{24}O_8S_{32}\cdot CH_3OH\cdot H_2O$	$C_{118}H_{94}B_2Ni_2N_{12}O_4S_{16}\cdot CH_3OH$	$C_{216}H_{168}B_4Co_4N_{24}O_8S_{16}\cdot CH_3OH\cdot 4H_2O$	$C_{109}H_{86}B_2Co_2N_{12}O_4S_8\cdot 1.5CH_3OH\cdot H_2O$	$C_{109}H_{86}B_2Ni_2N_{12}O_4S_8\cdot 2.5CH_3OH\cdot 1.25H_2O\cdot 0.5CH_2Cl_2$
M_r	514.70	4843.04	2428.09	4123.77	2089.94	2166.49
Crystal system	monoclinic	triclinic	triclinic	orthorhombic	triclinic	triclinic
Space group	$C2/c$	$P\bar{1}$	$P\bar{1}$	$P2_12_12_1$	$P\bar{1}$	$P\bar{1}$
a [Å]	38.298(2)	15.184(2)	10.8065(14)	10.1992(9)	15.2501(14)	15.1836(14)
b [Å]	5.8087(11)	19.962(3)	14.2625(18)	19.0998(18)	19.549(2)	19.5037(18)
c [Å]	25.3636(19)	20.389(3)	19.948(6)	55.654(2)	20.549(2)	20.5564(19)
α [°]	90	90.559(2)	94.148(2)	90	92.326(3)	92.772(2)
β [°]	126.991(3)	107.136(3)	95.399(3)	90	100.547(2)	100.249(2)
γ [°]	90	97.421(3)	106.735(2)	90	112.941(2)	112.780(2)
V [Å^3]	4506.8(10)	5848.7(15)	2915.2(10)	10841.5(15)	5503.7(9)	5476.8(9)
Z	8	1	1	2	2	2
ρ_c [g cm^{-3}]	1.517	1.375	1.383	1.263	1.261	1.314
$F(000)$	2128	2504	1258	4276	2170	2253
T [K]	291(2)	291(2)	291(2)	291(2)	291(2)	291(2)
μ(Mo-K_α) [mm^{-1}]	0.633	0.628	0.669	0.518	0.511	0.581
Index ranges	$-46 \le h \le 41$ $-7 \le k \le 7$ $-30 \le l \le 30$	$-14 \le h \le 18$ $-21 \le k \le 24$ $-25 \le l \le 25$	$-12 \le h \le 12$ $-16 \le k \le 13$ $-22 \le l \le 23$	$-12 \le h \le 12$ $-22 \le k \le 23$ $-68 \le l \le 41$	$-18 \le h \le 17$ $-23 \le k \le 17$ $-24 \le l \le 24$	$-17 \le h \le 18$ $-23 \le k \le 23$ $-15 \le l \le 24$
GOF (F^2)	0.991	1.038	1.021	1.051	1.016	0.999
R_1[a], wR_2[b] [$I > 2\sigma(I)$]	0.0583, 0.1157	0.0589, 0.1345	0.0506, 0.0920	0.0530, 0.1240	0.0842, 0.2149	0.0734, 0.1892
R_1[a], wR_2[b] (all data)	0.1003, 0.1242	0.0978, 0.1472	0.0860, 0.0998	0.0675, 0.1290	0.1997, 0.2351	0.1172, 0.2082

[a] $R_1 = \Sigma||C| - |F_c||/\Sigma F_o|$. [b] $wR_2 = [\Sigma w(F_o^2 - F_c^2)^2/\Sigma w(F_o^2)]^{1/2}$.

suggest that the ligand exists in the enol form in the solid state, and the H atom is localized mainly on O2.[12a] No obvious shorter S···S contacts are observed in the crystal structure, which is reasonable due to the intermolecular steric repulsions from the acetylacetonate groups.

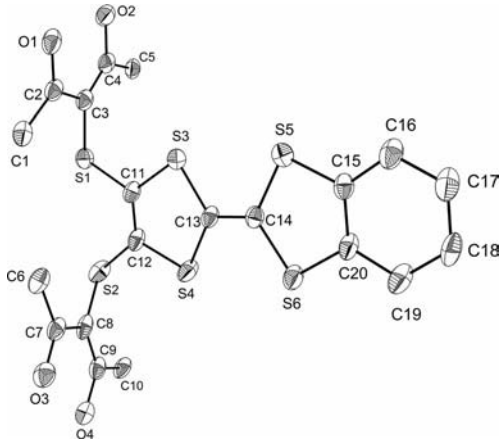

Figure 2. ORTEP view of $\mathbf{L_4}$ with the atom-numbering scheme. Thermal ellipsoids are drawn at 30% probability. Hydrogen atoms are omitted for clarity.

As shown in Figure 3, **2** is mononuclear. The central Ni^{II} ion is five-coordinate by two O atoms from the acetylacetonate unit and three N atoms from the capping Tp^{Ph_2} ligand, which forms a distorted tetragonal pyramidal, similar to Tp^{Ph_2}acac in ref.[20] The acetylacetonate unit coordinates to the Ni^{II} ion in a bidentate mode with Ni–O bond lengths of 1.951(2) and 1.958(2) Å. The Ni–N_{pz} bonds are not equivalent: Ni1–N3 [2.010(3) Å] is shorter than the other Ni–N bonds [2.054(2) for Ni1–N5 and 2.053(3) Å for Ni1–N1]. N1, N5, O1, and O2 form the basal plane and N3 occupies the apical position of the tetragonal pyramidal.

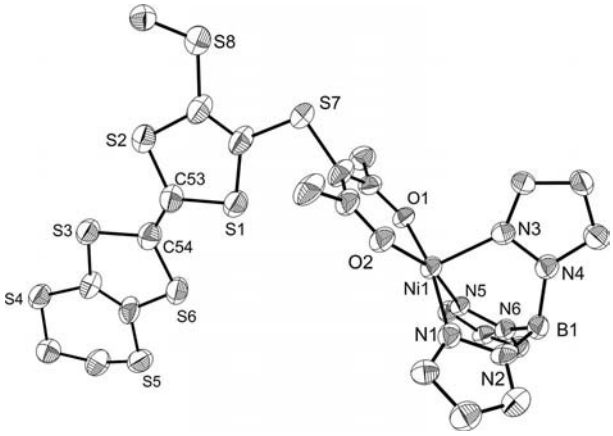

Figure 3. ORTEP view of **2** with the atom-numbering scheme. Thermal ellipsoids are drawn at 30% probability. Hydrogen atoms, solvated molecules, and phenyl rings are omitted for clarity.

Dinuclear **3**, **5**, and **6** have very similar structures. As shown in Figures 4, S2, and 5, the central metal ions have tetragonal pyramidal coordination geometry. The whole molecule looks like a lobster: the two acac groups form a pair of pincers that clamp the metal ions in a bidentate mode, and the TTF skeleton forms the body of the lobster. For **6**, the distance between the two Ni ions is 12.06 Å. It is noticeable that the TTF core adopts a boat-like configuation and the dihedral angle between the two five-membered rings is 26.68°. Neighboring lobster-like molecules form dimers in the structure with the shortest intermolecular S···S distance of 3.80 Å (Figure S3).

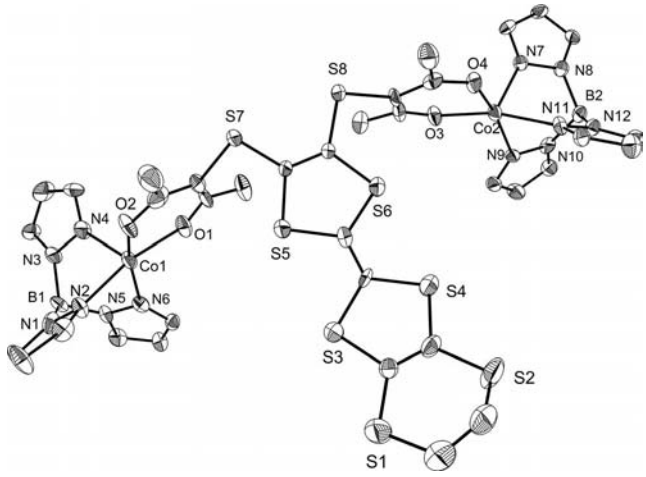

Figure 4. ORTEP view of **3** with the atom-numbering scheme. Thermal ellipsoids are drawn at 30% probability. Hydrogen atoms, solvated molecules, and phenyl rings are omitted for clarity.

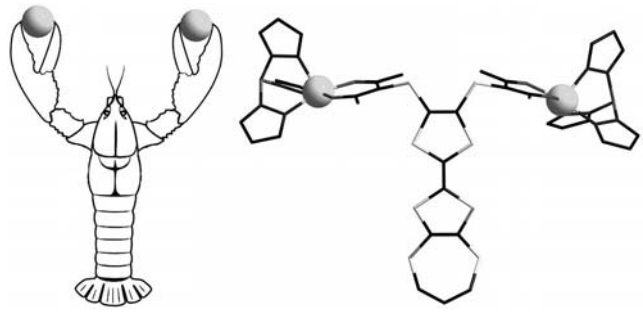

Figure 5. Crystal structure of **6** (right). Hydrogen atoms, solvated molecules, and phenyl rings are omitted for clarity.

Spectroscopic Properties

The UV/Vis spectra of $\mathbf{L_1}$–$\mathbf{L_4}$ and **1**–**8** in CH_2Cl_2 are shown in Figures 6 and S4–S6. The broad absorption bands at around 300 nm and the shoulder peak at around 330 nm in the spectra of $\mathbf{L_1}$–$\mathbf{L_4}$ are assigned to the characteristic π–π* transition of the TTF skeleton. In the spectra of **1**–**8**, the very intense absorption at ca. 245 nm may result from the Tp^{Ph_2} ligand. However, no obvious band with metal-to-ligand charge transfer (MLCT) character was observed. Upon addition of different amounts of $NOPF_6$, two broad absorption bands (420–520 and 800–1000 nm) emerged and their intensities increased gradually, suggesting the formation of charge-transfer complexes by oxidation of the electron-donating TTF unit.[21,25]

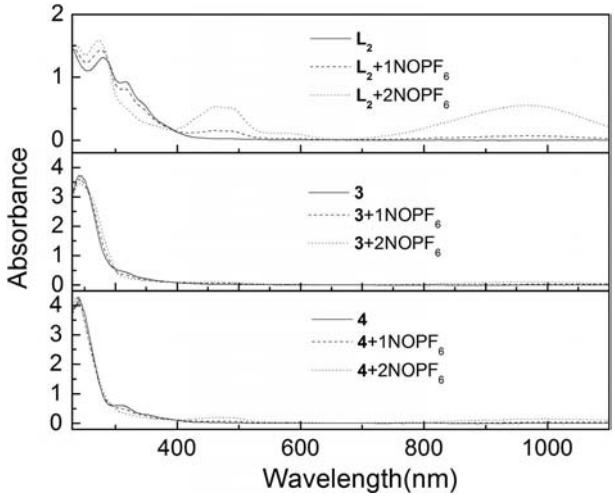

Figure 6. UV/Vis absorption spectra of **L_2**, **3**, and **4** (5×10^{-5} M) in the presence of varying amounts of $NOPF_6$ measured in CH_2Cl_2.

Electrochemical Properties

The electrochemical behavior of **L_1**–**L_4** and **1**–**8** were investigated in CH_2Cl_2 by cyclic voltammetry (Figures 7, S7–S9, and Table 5). As expected, **L_1**–**L_4** exhibit two reversible one-electron redox couples, the first ranging from 0.44 to 0.49 V and the second from 0.71 to 0.79 V, which are attributed to the formation of their radical cationic and dicationic species, respectively. Of the ligands, **L_4** displays the highest redox potentials, ca. 90 mV for $E_1^{1/2}$ and ca. 130 mV for $E_2^{1/2}$ higher than those of **L_1**–**L_3**. This is reasonable as there are less sulfur atoms in **L_4**, which makes it less delocalized and more difficult to oxidize in accordance with a previous report.[10]

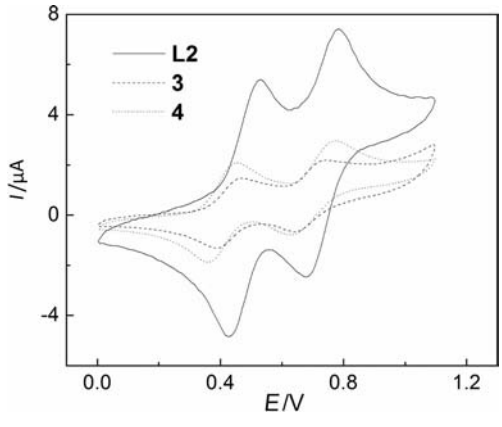

Figure 7. Cyclic voltammograms of **L_2**, **3**, and **4** (5×10^{-4} M) measured in CH_2Cl_2 at a scan rate of 100 mV s^{-1}.

Table 5. Cyclic voltammetry data [V] for **L_1**–**L_4** and **1**–**8**.

	$E^1_{1/2}$	$E^2_{1/2}$		$E^1_{1/2}$	$E^2_{1/2}$		$E^1_{1/2}$	$E^2_{1/2}$
L_1	0.461	0.741	**1**	0.429	0.720	**2**	0.413	0.721
L_2	0.479	0.732	**3**	0.424	0.688	**4**	0.408	0.701
L_3	0.441	0.717	**5**	0.429	0.699	**6**	0.408	0.699
L_4	0.491	0.788	**7**	0.462	0.782	**8**	0.436	0.776

Compared with **L_1**–**L_4**, **1**–**8** show lower potentials of both reversible single-electron oxidation waves, which indicates that electron transfer from Tp^{Ph_2} to TTF across the acetylacetonate bridge leads to an increase in the electronic density on the TTF moiety. As a result, they are easier to be oxidized to radical cations and dications than the noncoordinated ligands.[22] Of the four cobalt complexes, **8** exhibits the highest redox potentials, which indicates that it has the least delocalized structure. The $E_1^{1/2}$ values for the nickel complexes are lower than those of the corresponding cobalt complexes, whereas the $E_2^{1/2}$ values remain almost the same. However, compared with previous reports,[23] no redox peak is observed for the $Tp^{Ph_2}Co$ unit, which may arise from steric effects of the ligand that influence reversibility and the redox potential of the metal complex.

Magnetic Properties

Variable-temperature (T) magnetic susceptibility (χ_M) measurements were performed on polycrystalline samples of **3**–**8** in the range 1.8–300 K. As shown in Figures 8, 9, and S10–13, the main observation from the $\chi_M T$ vs. T curves for these complexes is that they are paramagnetic. For the cobalt complexes, at 300 K, the $\chi_M T$ values are 5.56 for **3**, 5.61 for **5**, and 5.56 $cm^3\,K\,mol^{-1}$ for **7**, which are significantly higher than the spin-only value of 3.75 $cm^3\,K\,mol^{-1}$ (g = 2.0) expected for two isolated high-spin Co^{II} (S = 3/2) ions. As the temperature decreases, the $\chi_M T$ value gradually decreases and reaches 3.70 for **3**, 4.65 for **5**, and 4.86 $cm^3\,K\,mol^{-1}$ for **7** at 70 K and then rapidly drops to 1.78 for **3**, 3.21 for **5**, and 3.49 $cm^3\,K\,mol^{-1}$

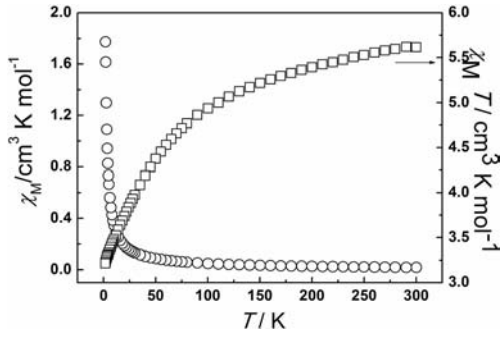

Figure 8. Temperature dependence of χ_M and $\chi_M T$ for **5** at 2 kOe.

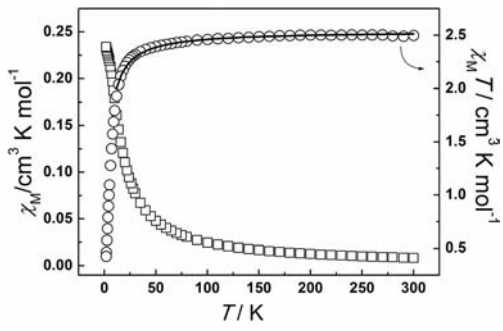

Figure 9. Temperature dependence of χ_M and χ_MT for **6** at 2 kOe.

for **7** at 1.8 K. This drastic decrease in $\chi_M T$ is mainly ascribed to the zero-field splitting (ZFS) of the octahedral high-spin Co^{II} ion.

For the Ni complexes, the $\chi_M T$ values are 2.62 for **4**, 2.49 for **6**, and 2.42 $cm^3 K mol^{-1}$ for **8** at 300 K, which is higher than the spin-only value of 2.0 $cm^3 K mol^{-1}$ (g = 2.0) of two Ni^{II} (S = 1) ions without any interaction. As the temperature decreases, the $\chi_M T$ values stay almost constant until 30 K and then rapidly drop to 0.43 for **4**, 0.42 for **6**, and 0.39 $cm^3 K mol^{-1}$ for **8** at 1.8 K, which is due to ZFS and/or intermolecular antiferromagnetic interactions. The $\chi_M T$ vs. T plots were fitted with Equation (1) from 300–12 K, and the best fit results are: g = 2.23, θ = –3.42 K for **4**; g = 2.25, θ = –3.18 K for **6**; and g = 2.22, θ = –3.43 K for **8**.

$$\chi_m T = 2 \times \frac{Ng^2\beta^2}{3k(T-\theta)} S(S+1)T \quad (1)$$

Computational Studies

In order to understand the nature of the electron absorption spectra of these coordination complexes, theoretical computations were carried out on **2**.

The optimized geometry of **2** conforms well to its crystal structure, although there are two apparent variations (Table 6). Firstly, different from the planar conformation in crystal, the TTF moiety becomes boat-like with a dihedral angle of ca. 50° in the optimized molecule. Moreover, after optimization, the coordinating atoms around the Ni atom form a tetragonal pyramidal conformation, but the Ni1–N3 bond elongates from 201 to 269 pm, and the bond lengths between Ni and other coordinating atoms are all shortened by about 15 pm. Such variation may indicate that the Ni^{II} ion prefers to be four- rather than five-coordinate in solution.

Table 6. Comparison of selected bond lengths of **2** [Å].

	Exp.	Calcd.
Ni1–N3	2.01	2.69
Ni1–N1	2.05	1.91
Ni1–N5	2.05	1.90
Ni1–O1	1.95	1.84
Ni1–O2	1.96	1.84

As shown in Table 7 and Figure 10, the results of the TD-DFT calculation are in good agreement with the experimental data.[24] According to the calculated molecular orbital graphs (Figure 11) and electron density distribution (Table 8, Scheme 3), the intense absorption band at around 319 nm can be assigned to ligand-to-ligand charge transfer (LLCT) from TTF–acac to Tp^{Ph_2} [highest occupied molecular orbital (HOMO)→lowest unoccupied molecular orbital (LOMO)+6], whereas the weaker absorption band at about 342 nm also has LLCT character between Tp^{Ph_2} and TTF–acac (HOMO→LOMO+8 and HOMO-2→LOMO+2). On the other hand, the shoulder band at around 368 nm is due to intramolecular charge transfer (ICT) from the π orbital of the TTF moiety to the π* orbital of the acac moiety, which reveals a π→π*-type transition (HOMO→LOMO+5). It is noteworthy that very weak charge transfer between the metal and ligands, i.e. MLCT

Table 7. Main experimental and calculated electronic transitions of **2**.

Exp. [nm]	Calcd. [nm]	f[a]	Character	Orbital excitations
368	362	0.0703	ICT	H→L+5 (88%)
346	342	0.1394	LLCT	H→L+8 (39%), H-2→L+2 (20%)
313	319	0.1337	LLCT	H→L+6 (52%)

[a] Oscillator strength.

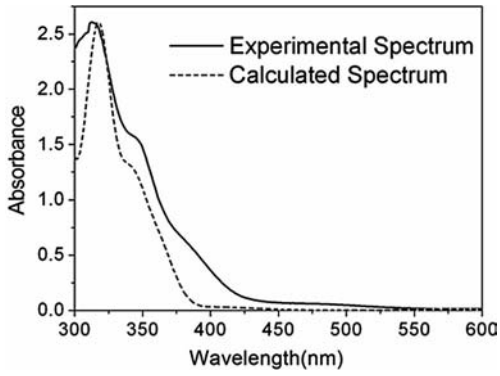

Figure 10. Experimental and calculated absorption spectra of **2** in the range of 300–600 nm.

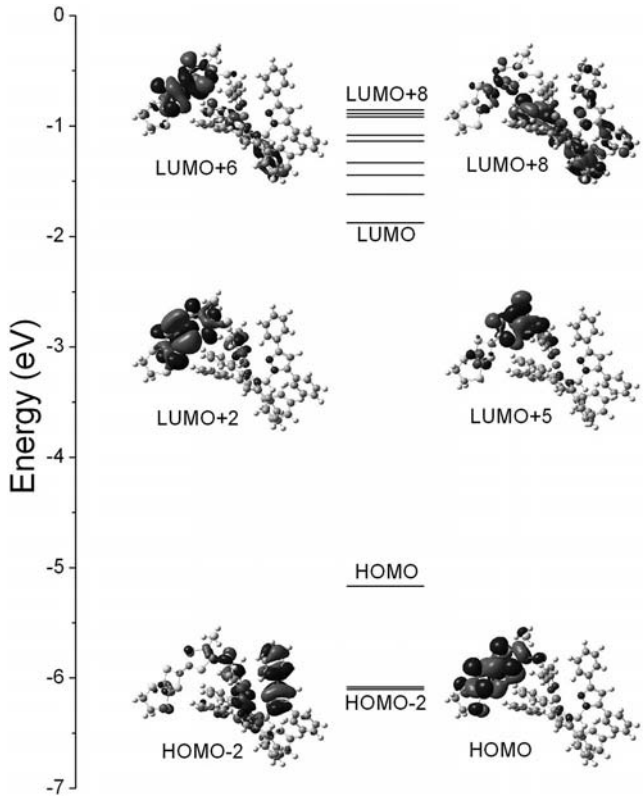

Figure 11. Molecular orbital energy level and graphical representation of transition-related molecular orbitals of **2**.

and ligand-to-metal charge transfer, can be observed both in the experiment and calculation, which indicates that there is a low possibility for the occurrence of such transitions. This is probably due to the large energy gap between the frontier molecular orbitals of Ni^{II} and the ligands.

Table 8. Electron density distribution of the transition-related orbitals of **2** (see Scheme 3).

Orbital	Energy [eV]	Composition [%]			
		TTF	acac	Ni	Tp^{Ph_2}
LUMO+8	–0.854	43.1	26.5	4.5	25.9
LUMO+6	–0.916	15.9	11.8	0.6	71.7
LUMO+5	–1.081	30.7	32.4	3.0	33.9
LUMO+2	–1.442	86.1	1.8	0.2	12.0
HOMO	–5.167	46.8	16.2	0.4	36.6
HOMO–2	–6.106	41.5	10.7	2.9	45.0

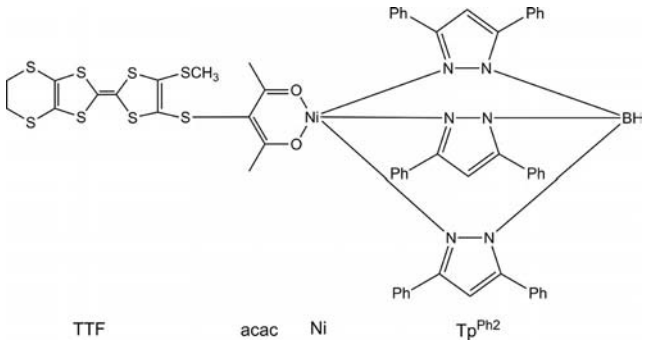

Scheme 3. Representative scheme of four moieties of **2**.

Conclusions

A series of TTF-acetylacetonate ligands has been prepared, and their coordination capability has been confirmed by the formation of Co/Ni complexes. The complexes have highly conjugated structures and show interesting redox properties. Theoretical calculations were carried out to determine the nature of the electron absorption phenomena. The results indicate that the acetylacetonate bridge is a useful linkage for the synthesis and design of new multifunctional materials. Further investigations will focus on the charge transfer properties and exploring interesting conducting and magnetic materials.

Experimental Section

General Procedures: Schlenk techniques were used to carry out manipulations under a N_2 atmosphere. IR spectra were measured with a Vector 22 Bruker spectrophotometer (400–4000 cm^{-1}) as KBr pellets. Absorption spectra were measured with a Shimadzu UV-3100 spectrophotometer. Elemental analyses for C, H, and N were performed with a Perkin–Elmer 240C analyzer. Cyclic voltammetry was performed with an IM6ex electrochemical workstation with platinum as the working and counter electrodes, Ag/Ag^+ as the reference electrode, and 0.1 M n-Bu_4NClO_4 as the supporting electrolyte. NMR spectra were measured with a Bruker AM 500 spectrometer. Mass spectra were recorded with a Bruker Autoflex II TM instrument for MALDI-TOF MS. $\mathbf{L_1}$,[25] 2,3-bis(cyanoethylthio)-6,7-ethylenedithio-1,4,5,8-tetrathiafulvalene,[26] $(Tp^{Ph_2})Co(OAc)(Hpz^{Ph_2})$,[27] and $(Tp^{Ph_2})Ni(OAc)$[28] were synthesized in high yields according to literature methods. 2,3-Bis(cyanoethylthio)-6,7-propylenedithio-1,4,5,8-tetrathiafulvalene and 2,3-bis(cyanoethylthio)-6,7-benzo-1,4,5,8-tetrathiafulvalene were synthesized by a similar method to 2,3-bis(cyanoethylthio)-6,7-ethylenedithio-1,4,5,8-tetrathiafulvalene.

Ligand L_2: Under a nitrogen atmosphere, to a solution of 2,3-bis(cyanoethylthio)-6,7-ethylenedithio-1,4,5,8-tetrathiafulvalene (651 mg, 1.4 mmol) in THF (25 mL) was added dropwise a solution of $CsOH·H_2O$ (503 mg, 3.0 mmol) in CH_3OH (6 mL) at room temperature. The mixture was allowed to stir for 30 min before 3-chloro-2,4-pentanedione (0.45 mL, 4.0 mmol) was added. The reaction mixture was stirred overnight. The solvent was removed, and the orange residue was extracted into CH_2Cl_2 and washed with water. The organic extract was purified by column chromatography (CH_2Cl_2/petroleum ether) on silica gel (yield: 465 mg, 60%). IR (KBr): $\tilde{\nu}$ = 3415, 2921, 1551, 1402, 1286, 1010, 893, 766 cm^{-1}. ^1H NMR (500 MHz, $CDCl_3$): δ = 2.50 (s, 12 H), 3.31 (t, 4 H) 17.24 (s, 2 H) ppm. MS (MALDI-TOF): m/z = 553.9 $[M – H]^+$. $C_{18}H_{18}O_4S_6$ (490.70): calcd. C 38.96, H 3.27; found C 38.91, H 3.23.

Ligand L_3: Orange $\mathbf{L_3}$ was obtained according to the method described above for $\mathbf{L_2}$. Yield: 450 mg, 57%. IR (KBr): $\tilde{\nu}$ = 3419, 2923, 2853, 1567, 1398, 1273, 1013, 900, 769 cm^{-1}. ^1H NMR (500 MHz, $CDCl_3$): δ = 2.41 (m, 2 H), 2.49 (s, 12 H), 2.70 (t, 4 H), 17.24 (s, 2 H) ppm. MS (MALDI-TOF): m/z = 568.0 $[M – H]^+$. $C_{19}H_{20}O_4S_8$ (568.84): calcd. C 40.11, H 3.54; found C 40.25, H 3.47.

Ligand L_4: $\mathbf{L_4}$ was obtained according to the method described above for $\mathbf{L_2}$. Yield: 502 mg, 71%. IR (KBr): $\tilde{\nu}$ = 3421, 2921, 1569, 1400, 1254, 1011, 905, 769, 731 cm^{-1}. ^1H NMR (500 MHz, $CDCl_3$): δ = 2.51 (s, 12 H), 7.12 (d, 2 H), 7.24 (t, 2 H), 17.25 (s, 2 H) ppm. MS (MALDI-TOF): m/z = 513.8 $[M – H]^+$. $C_{18}H_{20}O_4S_6$ (492.71): calcd. C 46.67, H 3.52; found C 46.79, H 3.58.

$Tp^{Ph_2}CoL_1·CH_3OH·H_2O$ (1): To a solution of $(Tp^{Ph_2})Co(OAc)(Hpz^{Ph_2})$ (20.1 mg, 0.02 mmol) in a mixture of CH_2Cl_2/CH_3OH (3 mL/2 mL) was slowly added a solution of $\mathbf{L_1}$ (10.1 mg, 0.02 mmol) in CH_2Cl_2 (8 mL). Single crystals suitable for X-ray structure determination were obtained by slow evaporation after several days. Yield: 81%. IR (KBr): $\tilde{\nu}$ = 3415, 2917, 1645, 1567, 1477, 1460, 1363, 1166, 1063, 760, 696 cm^{-1}. $C_{59}H_{47}BCoN_6O_2S_8$ (1198.28): calcd. C 59.14, H 3.96, N 7.01; found C 59.02, H 3.95, N 7.11.

$Tp^{Ph_2}NiL_1·CH_3OH$ (2): To a solution of $(Tp^{Ph_2})Ni(OAc)$ (16.2 mg, 0.02 mmol) in a mixture of CH_2Cl_2/CH_3OH (3 mL/2 mL) was slowly added a solution of $\mathbf{L_1}$ (10.1 mg, 0.02 mmol) in CH_2Cl_2 (8 mL). Single crystals suitable for X-ray structure determination were obtained by slow evaporation after several days. Yield: 77%. IR (KBr): $\tilde{\nu}$ = 3415, 2920, 1665, 1570, 1477, 1460, 1366, 1167, 1063, 758, 695 cm^{-1}. $C_{59}H_{47}BN_6NiO_2S_8$ (1198.06): calcd. C 59.15, H 3.95, N 7.01; found C 59.08, H 3.88, N 6.94.

$(Tp^{Ph_2}Co)_2L_2·CH_3OH·4H_2O$ (3): Complex **3** was obtained according to the method described above for **1**. Yield: 53%. IR (KBr): $\tilde{\nu}$ = 3418, 2915, 1568, 1477, 1461, 1363, 1171, 1066, 758, 696 cm^{-1}. $C_{108}H_{84}B_2Co_2N_{12}O_4S_8$ (2009.90): calcd. C 64.54, H 4.21, N 8.36; found C 64.37, H 4.35, N 8.34.

$(Tp^{Ph_2}Ni)_2L_2$ (4): Complex **4** was obtained according to the method described above for **2**. Yield: 46%. IR (KBr): $\tilde{\nu}$ = 3418, 2916, 1570, 1477, 1462, 1366, 1171, 1067, 760, 695 cm^{-1}. $C_{108}H_{84}B_2N_{12}Ni_2O_4S_8$

(2009.45): calcd. C 64.55, H 4.21, N 8.36; found C 64.47, H 4.30, N 8.28.

$(Tp^{Ph_2}Co)_2L_3\cdot 1.5CH_3OH\cdot H_2O$ (5): Complex **5** was obtained according to the method described above for **1**. Yield: 54%. IR (KBr): $\tilde{\nu}$ = 3416, 2921, 1568, 1476, 1460, 1410, 1362, 1169, 1063, 760, 695 cm^{-1}. $C_{109}H_{86}B_2Co_2N_{12}O_4S_8$ (2023.92): calcd. C 64.68, H 4.28, N 8.30; found C 64.54, H 4.20, N 8.19.

$(Tp^{Ph_2}Ni)_2L_3\cdot 2.5CH_3OH\cdot 1.25H_2O\cdot 0.5CH_2Cl_2$ (6): Complex **6** was obtained according to the method described above for **2**. Yield: 50%. IR (KBr): $\tilde{\nu}$ = 3419, 2921, 1574, 1477, 1460, 1366, 1169, 1066, 759, 695 cm^{-1}. $C_{109}H_{86}B_2N_{12}Ni_2O_4S_8$ (2023.48): calcd. C 64.70, H 4.28, N 8.31; found C 64.59, H 4.25, N 8.16.

$(Tp^{Ph_2}Co)_2L_4$ (7): Complex **7** was obtained according to the method described above for **1**. Yield: 55%. IR (KBr): $\tilde{\nu}$ = 3415, 2921, 1569, 1477, 1461, 1362, 1168, 1065, 760, 695 cm^{-1}. $C_{110}H_{84}B_2Co_2N_{12}O_4S_6$ (1969.80): calcd. C 67.07, H 4.30, N 8.53; found C 66.92, H 4.25, N 8.46.

$(Tp^{Ph_2}Ni)_2L_4$ (8): Complex **8** was obtained according to the method described above for **2**. Yield: 54%. IR (KBr): $\tilde{\nu}$ = 3420, 2921, 1573, 1478, 1461, 1366, 1170, 1066, 760, 695 cm^{-1}. $C_{110}H_{84}B_2N_{12}Ni_2O_4S_6$ (1969.35): calcd. C 67.09, H 4.30, N 8.53; found C 67.17, H 4.27, N 8.60.

Crystal Structure Determination: Data were collected with a Bruker Smart Apex CCD diffractometer equipped with graphite-monochromated Mo-K_α (λ = 0.71073 Å) radiation using a ω-2θ scan mode at 293 K. The highly redundant data sets were reduced using SAINT[29] and corrected for Lorentz and polarization effects. Absorption corrections were applied using SADABS.[30] The structure was solved by direct methods and refined by full-matrix least-squares methods on F^2 using SHELXTL-97.[31] All non-hydrogen atoms were found in alternating difference Fourier syntheses and least-squares refinement cycles and, during the final cycles, refined anisotropically. Hydrogen atoms were placed in calculated positions and refined as riding atoms with a uniform value of U_{iso}.

CCDC-818340 (for $\mathbf{L_4}$), 818341 (for **1**), 818342 (for **2**), 818343 (for **3**), 818344 (for **5**), and 818345 (for **6**) contain the supplementary crystallographic data for this paper. These data can be obtained free of charge from The Cambridge Crystallographic Data Centre via www.ccdc.cam.ac.uk/data_request/cif.

Computational Details: Calculations were performed using the Gaussian 03 Program Package.[32] We employed DFT and TD-DFT with no symmetry constraints to investigate the optimized geometry, electron configuration, and electronic absorption spectrum of **2** with three-parameter hybrid functional (B3LYP)[33] and utilized 6-31+G (d) as the basis set for all the atoms. A conductor-like polarized continuum model approach was performed to consider the influence of solvent molecules (dichloromethane in this case) on the geometry and electronic configuration.

Supporting Information (see footnote on the first page of this article): ORTEP views of **1** and **5**; crystal structure of **6**; UV/Vis spectra of $\mathbf{L_1}$, **1**, **2**, $\mathbf{L_3}$, **5**, **6**, $\mathbf{L_4}$, **7**, and **8**; cyclic voltammograms of $\mathbf{L_1}$–$\mathbf{L_4}$, **1**, **3**, **5**, **7**, **2**, **4**, **6**, and **8**; temperature dependence of χ_M and $\chi_M T$ of **3**, **7**, **4**, and **8**; bond lengths and angles of **1**, **3**, and **5**.

Acknowledgments

This work was supported by the Major State Basic Research Development Program (grant numbers 2007CB925103 and 2011CB808704), the National Science Fund for Distinguished Young Scholars of China (grant number 20725104), and the National Natural Science Foundation of China (NSFC) (grant numbers 91022031 and 21021062).

[1] a) P. Day, M. Kurmoo, T. Mallah, I. R. Marsden, R. H. Friend, F. L. Pratt, W. Hayes, D. Chasseau, J. Gaultier, G. Bravic, L. Ducasse, *J. Am. Chem. Soc.* **1992**, *114*, 10772–10773; b) E. Coronado, P. Day, *Chem. Rev.* **2004**, *104*, 5419–5448; c) E. Coronado, J. R. Galan-Mascaros, C. J. Gomez-Garcia, V. Laukhin, *Nature* **2000**, *408*, 447–449.

[2] a) H. Kobayashi, A. Kobayashi, P. Cassoux, *Chem. Soc. Rev.* **2000**, *29*, 325–333; b) A. Kobayashi, E. Fijiwara, H. Kobayashi, *Chem. Rev.* **2004**, *104*, 5243–5264; c) T. Enoki, A. Miyasaki, *Chem. Rev.* **2004**, *104*, 5449–5477; d) H. Fujiwara, K. Wada, T. Hiraoka, T. Hayashi, T. Sugimoto, H. Nakazumi, K. Yokogawa, M. Teramura, S. Yasuzuka, K. Murata, T. Mori, *J. Am. Chem. Soc.* **2005**, *127*, 14166–14167.

[3] a) S. Uji, H. Shinagawa, T. Terashima, C. Terakura, T. Yakabe, Y. Terai, M. Tokumoto, A. Kobayashi, H. Tanaka, H. Kobayashi, *Nature* **2001**, *410*, 908–910; b) F. Pointillart, O. Maury, Y. Le Gal, S. Golhen, O. Cador, L. Ouahab, *Inorg. Chem.* **2009**, *48*, 7421–7429; c) F. Pointillart, Y. Le Gal, S. Golhen, O. Cador, L. Ouahab, *Inorg. Chem.* **2008**, *47*, 9730–9732.

[4] a) M. Bendikov, F. Wudl, D. F. Perepichka, *Chem. Rev.* **2004**, *104*, 4891–4945; b) H. Kobayashi, H. Cui, A. Kobayashi, *Chem. Rev.* **2004**, *104*, 5265–5288.

[5] a) M. Shatruk, L. Ray, *Dalton Trans.* **2010**, 11105–11121; b) D. Lorcya, N. Belleca, M. Fourmiguéa, N. Avarvari, *Coord. Chem. Rev.* **2009**, *253*, 1398–1438.

[6] H. R. Wen, C. H. Li, Y. Song, J. L. Zuo, B. Zhang, X. Z. You, *Inorg. Chem.* **2007**, *46*, 6837–6839.

[7] a) M. Kumasaki, H. Tanaka, A. Kobayashi, *J. Mater. Chem.* **1998**, *8*, 301–307; b) H. Tanaka, M. Tokumoto, S. Ishibashi, D. Graf, E. S. Choi, J. S. Brooks, S. Yasuzuka, Y. Okano, H. Kobayashi, A. Kobayashi, *J. Am. Chem. Soc.* **2004**, *126*, 10518–10519; c) E. Fujiwara, A. Kobayashi, H. Fujiwara, H. Kobayashi, *Inorg. Chem.* **2004**, *43*, 1122–1129.

[8] a) F. Pointillart, O. Maury, Y. Le Gal, S. Golhen, O. Cador, L. Ouahab, *Inorg. Chem.* **2009**, *48*, 7421–7429; b) F. Pointillart, T. Cauchy, Y. Le Gal, S. Golhen, O. Cador, L. Ouahab, *Inorg. Chem.* **2010**, *49*, 1947–1960; c) N. Benbellat, K. S. Gavrilenko, Y. Le Gal, O. Cador, S. Golhen, A. Gouasmia, J. M. Fabre, L. Ouahab, *Inorg. Chem.* **2006**, *45*, 10440–10442; d) F. Setifi, L. Ouahab, S. Golhen, Y. Yoshida, G. Saito, *Inorg. Chem.* **2003**, *42*, 1791–1793.

[9] a) S. X. Liu, S. Dolder, P. Franz, A. Neels, H. Stoeckli-Evans, S. Decurtins, *Inorg. Chem.* **2003**, *42*, 4801–4803; b) S. X. Liu, S. Dolder, M. Pilkington, S. Decurtins, *J. Org. Chem.* **2002**, *67*, 3160–3162; c) T. Devic, N. Avarvari, P. Batail, *Chem. Eur. J.* **2004**, *10*, 3697–3707.

[10] W. Liu, J. Xiong, Y. Wang, X. H. Zhou, R. Wang, J. L. Zuo, X. Z. You, *Organometallics* **2009**, *28*, 755–762.

[11] a) S. Ichikawa, S. Kimura, H. Mori, G. Yoshida, H. Tajima, *Inorg. Chem.* **2006**, *45*, 7575–7577; b) C. Jia, S. X. Liu, C. Tanner, C. Leiggener, A. Neels, L. Sanguinet, E. Levillain, S. Leutwyler, A. Hauser, S. Decurtins, *Chem. Eur. J.* **2007**, *13*, 3804–3812; c) L. K. Keniley, L. Ray, K. Kovnir, L. A. Dellinger, J. M. Hoyt, M. Shatruk, *Inorg. Chem.* **2010**, *49*, 1307–1309.

[12] a) N. Avarvari, M. Fourmigué, *Chem. Commun.* **2004**, 1300–1301; b) G. Gachot, P. Pellon, T. Roisnel, D. Lorcy, *Eur. J. Inorg. Chem.* **2006**, 2604–2611; c) C. E. Uzelmeier, B. W. Smucker, E. W. Reinheimer, M. Shatruk, A. W. O'Neal, M. Fourmigué, K. R. Dunbar, *Dalton Trans.* **2006**, 5259–5268; d) K. S. Shin, Y. Jung, S. K. Lee, M. Fourmigué, F. Barrière, J. F. Bergamini, D. Y. Noh, *Dalton Trans.* **2008**, 5869–5871.

[13] a) T. L. A. Nguyen, R. Demir-Cakan, T. Devic, M. Morcrette, T. Ahnfeldt, P. Auban-Senzier, N. Stock, A. M. Goncalves, Y. Filinchuk, J. M. Tarascon, G. Férey, *Inorg. Chem.* **2010**, *49*, 7135–7143; b) M. Ebihara, M. Nomura, S. Sakai, T. Kawamura, *Inorg. Chim. Acta* **2007**, *360*, 2345–2352; c) J. Gu, Q. Y.

Zhu, Y. Zhang, W. Lu, G. Y. Niu, J. Dai, *Inorg. Chem. Commun.* **2008**, *11*, 175–178.
[14] a) J. Massue, N. Bellec, S. Chopin, E. Levillain, T. Roisnel, R. Clérac, D. Lorcy, *Inorg. Chem.* **2005**, *44*, 8740–8748; b) N. Bellec, J. Massue, T. Roisnel, D. Lorcy, *Inorg. Chem. Commun.* **2007**, *10*, 1172–1176; c) N. Bellec, D. Lorcy, *Tetrahedron Lett.* **2001**, *42*, 3189–3191; d) Y. J. Li, W. Liu, Y. Z. Li, J. L. Zuo, X. Z. You, *Inorg. Chem. Commun.* **2008**, *11*, 1466–1473.
[15] J. C. Wu, S. X. Liu, T. D. Keene, A. Neels, V. Mereacre, A. K. Powell, S. Decurtins, *Inorg. Chem.* **2008**, *47*, 3452–3459.
[16] S. Trofimenko, *Chem. Rev.* **1993**, *93*, 943–980.
[17] a) S. Trofimenko, J. C. Calabrese, J. K. Kochi, S. Wolowiec, F. B. Hulsbergen, J. Reedijk, *Inorg. Chem.* **1992**, *31*, 3943–3950; b) S. Trofimenko, J. C. Calabrese, J. S. Thompson, *Inorg. Chem.* **1989**, *28*, 1091–1101; c) S. Trofimenko, J. C. Calabrese, P. J. Domaille, J. S. Thompson, *Inorg. Chem.* **1987**, *26*, 1507–1510.
[18] a) C. Bergquist, T. Fillebeen, M. M. Morlok, G. Parkin, *J. Am. Chem. Soc.* **2003**, *125*, 6189–6197; b) N. Shirasawa, T. T. Nguyet, S. Hikichi, Y. Moro-oka, M. Akita, *Organometallics* **2001**, *20*, 3582–3598; c) N. Shirasawa, M. Akita, S. Hikichi, Y. Moro-oka, *Chem. Commun.* **1999**, 417–434; d) A. S. Yakovenko, S. V. Kolotilov, A. W. Addison, S. Trofimenko, G. P. A. Yap, V. Lopushanskaya, V. V. Pavlishchuk, *Inorg. Chem. Commun.* **2005**, *8*, 932–935.
[19] a) P. Pellon, G. Gachot, J. Le Bris, S. Marchin, R. Carlier, D. Lorcy, *Inorg. Chem.* **2003**, *42*, 2056–2060; b) Q. Y. Zhu, G. Q. Bian, Y. Zhang, J. Dai, D. Q. Zhang, W. Lu, *Inorg. Chim. Acta* **2006**, *359*, 2303–2308.
[20] D. J. Harding, P. Harding, H. Adams, *Trans. Met. Chem.* **2011**, *36*, 249–254.
[21] a) W. Sun, C. H. Xu, Z. Zhu, C. J. Fang, C. H. Yan, *J. Phys. Chem. C* **2008**, *112*, 16973–16983; b) Y. Zhou, H. Wu, L. Qu, D. Q. Zhang, D. B. Zhu, *J. Phys. Chem. B* **2006**, *110*, 15676–15679; c) F. Dumur, N. Gautier, N. Gallego-Planas, Y. Sahin, E. Levillain, N. Mercier, P. Hudhomme, M. M. A. Girlando, V. Lloveras, J. Vidal-Gancedo, J. Veciana, C. Rovira, *J. Org. Chem.* **2004**, *69*, 2164–2177; d) Y. F. Ran, C. Bluma, S. X. Liu, L. Sanguinet, E. Levillain, S. Decurtins, *Tetrahedron* **2011**, *67*, 1623–1627; e) R. Wang, L. C. Kang, J. Xiong, X. W. Dou, X. Y. Chen, J. L. Zuo, X. Z. You, *Dalton Trans.* **2011**, *40*, 919–926.
[22] a) F. Pointillart, Y. Le Gal, S. Golhen, O. Cador, L. Ouahab, *Inorg. Chem.* **2009**, *48*, 4631–4633; b) G. Prabusankar, Y. Molard, S. Cordier, S. Golhen, Y. Le Gal, C. Perrin, L. Ouahab, S. Kahlal, J. F. Halet, *Eur. J. Inorg. Chem.* **2009**, 2153–2161.
[23] D. J. Harding, P. Harding, R. Daengngern, S. Yimklan, H. Adams, *Dalton Trans.* **2009**, 1314–1320.
[24] N. M. O'Boyle, A. L. Tenderholt, K. M. Langner, *J. Comput. Chem.* **2008**, *29*, 839–845.
[25] C. H. Xu, W. Sun, C. Zhang, C. Zhou, C. J. Fang, C. H. Yan, *Chem. Eur. J.* **2009**, *15*, 8717–8721.
[26] N. Svenstrup, K. M. Rasmussen, T. K. Hansen, J. Becher, *Synthesis* **1994**, *8*, 809–812.
[27] D. J. Harding, H. Adams, T. Tuntulani, *Acta Crystallogr., Sect. C* **2005**, *61*, m301–m303.
[28] D. J. Harding, P. Harding, H. Adams, T. Tuntulani, *Inorg. Chim. Acta* **2007**, *360*, 3335–3340.
[29] *SAINT-Plus*, version 6.02, Bruker Analytical X-ray System, Madison, WI, **1999**.
[30] G. M. Sheldrick, SADABS, *An empirical absorption correction program*, Bruker Analytical X-ray Systems, Madison, WI, **1996**.
[31] G. M. Sheldrick, *SHELXTL-97*, University of of Göttingen, Germany, **1997**.
[32] M. J. Frisch, G. W. Trucks, H. B. Schlegel, G. E. Scuseria, M. A. Robb, J. R. Cheeseman, J. A. Montgomery, T. Vreven, K. N. Kudin, J. C. Burant, J. M. Millam, S. S. Iyengar, J. Tomasi, V. Barone, B. Mennucci, M. Cossi, G. Scalmani, N. Rega, G. A. Petersson, H. Nakatsuji, M. Hada, M. Ehara, K. Toyota, R. Fukuda, J. Hasegawa, M. Ishida, T. Nakajima, Y. Honda, O. Kitao, H. Nakai, M. Klene, X. Li, J. E. Knox, H. P. Hratchian, J. B. Cross, V. Bakken, C. Adamo, J. Jaramillo, R. Gomperts, R. E. Stratmann, O. Yazyev, A. J. Austin, R. Cammi, C. Pomelli, J. Ochterski, P. Y. Ayala, K. Morokuma, G. A. Voth, P. Salvador, J. J. Dannenberg, V. G. Zakrzewski, S. Dapprich, A. D. Daniels, M. C. Strain, O. Farkas, D. K. Malick, A. D. Rabuck, K. Raghavachari, J. B. Foresman, J. V. Ortiz, Q. Cui, A. G. Baboul, S. Clifford, J. Cioslowski, B. B. Stefanov, G. Liu, A. Liashenko, P. Piskorz, I. Komaromi, R. L. Martin, D. J. Fox, T. Keith, M. A. Al-Laham, C. Y. Peng, A. Nanayakkara, M. Challacombe, P. M. W. Gill, B. G. Johnson, W. Chen, M. W. Wong, C. Gonzalez, J. A. Pople, *Gaussian 03*, revision B.04, Gaussian, Inc., Wallingford, CT, **2004**.
[33] a) C. Lee, W. Yang, R. G. Parr, *Phys. Rev. B* **1988**, *37*, 785–789; b) B. Miehlich, A. Savin, H. Stoll, H. Preuss, *Chem. Phys. Lett.* **1989**, *157*, 200–206; c) A. D. Becke, *J. Chem. Phys.* **1993**, *98*, 5648–5652.

Received: June 21, 2011
Published Online: October 14, 2011

